

A 100-1600 MEV HIGH CURRENT SC PROTON LINAC FOR WASTE TRANSMUTATION AND ENERGY AMPLIFICATION

C. Pagani, G. Bellomo, P. Pierini,

D. Barni, A. Bosotti, A. Martino, R. Parodi*, S. Visonà

INFN Sezione di Milano, LASA, Via Fratelli Cervi 201, 20090 Segrate (MI), Italy

**INFN Sezione di Genova, Via Dodecaneso 33, 16146 Genova, Italy*

Abstract

An R&D program has started in Italy on an accelerator driven system for nuclear waste transmutation. The large flux of spallation neutrons from a high current CW proton linac accelerator is intended to drive a subcritical system to transmute nuclear waste, while producing energy. Our specific task is to develop, together with the national industry, a design of the high energy part of the proton accelerator, along with prototype development for its most critical components. In this paper we report the present design status, that follows from the design proposed at Linac'96 and revised at PAC'97. A 1.6 GeV linac, operated at 25 mA, allows to reach 40 MW of beam power. A beam power upgrade is achievable using additional couplers per cavity.

Introduction

The design criteria of the superconducting linac for the high energy section (100-1600 MeV) of the ADS (Accelerator Driven System) project has been presented both at the Linac 96[1] and at the PAC 97[2] Conferences. This design is based on a three section linac using elliptical cavities at the 350 MHz LEP frequency. The low energy part of the proposed machine consists of a proton source[3], a 350 MHz RFQ and a room temperature[4] (or SC[5]) DTL linac up to 100 MeV.

The three sections of the linac will use five cell cavities, designed to match the proton beam at the normalized velocities $\beta=0.5$, 0.65 and 0.85. The focusing will be provided by a quadrupole doublet structure, and the cavity cryostats will be placed in the space between two doublets. To account for the need for stronger focusing at low energies, the focusing periods of the three sections will accommodate two, three and four cavities, respectively. The nominal energy at the end of the linac is 1.6 GeV, delivering a 40 MW beam power at 25 mA beam current. A beam power upgrade is achievable using one or more additional couplers per cavity, while the energy could be increased to 1.7 GeV at the constant energy gain of 10 MeV/cavity (see Fig. 1).

General Layout

Each linac section consist of a cryomodule, separated by a 3 meter intermodule distance to accommodate the quadrupole doublet, the steering magnets, a diagnostic station and a pumping box. The beam pipe aperture is kept at a radius larger than 10 cm through the whole linac, to take advantage of the large aperture of the low frequency cavities, while using standard CF200 flanges.

A singlet (FODO) focusing scheme would lead to a cost increase either from additional cold/warm transitions or from the requirements of superconducting quadrupoles. The doublet scheme is more compact and allows longer cryomodules, which increase the “real estate” gradient of the linac.

Due to the reduced length and volume, the low β cavities tend to have greater surface electric and magnetic fields (relative to the same accelerating field seen by the particle) with respect to the $\beta=1$ structures. Therefore, we chose smaller accelerating gradients (and energy gain per cavity) in the first two sections of the linac. In order to select the cavity geometry and operating point, we required the maximum surface field on the cavity to be smaller than 15 MV/m and the peak magnetic field to be smaller than 40 mT. These values are conservative, being within the limits of the operational experience of the LEP2 cavities. The energy gain per cavity as a function of the linac energy is shown in Fig. 1, compared with the maximum energy gain for a peak surface field of 15 MV/m. In the first few periods of each section the energy gain per cavity is increased to a maximum value. The majority of the $\beta=0.85$ cavities operate at the energy gain of 10 MeV per cavity. To deliver such an energy gain to a 25 mA beam, a power coupler able to deliver 250 kW is required[6].

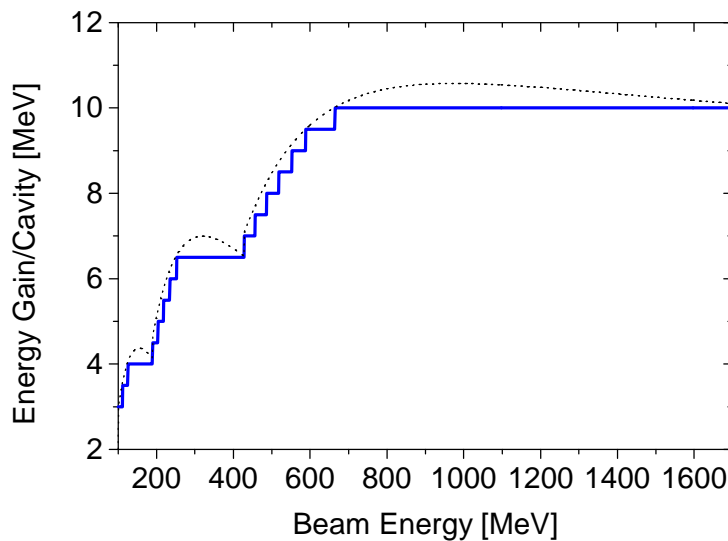


Figure 1. The energy gain per cavity along the three sections of the accelerator. The upper (dotted) curve is the nominal energy gain for a maximum peak surface field of 15 MV/m. The lower curve is the actual energy gain in our design.

The nominal power of 1 MW out of the existing 1.3 MW CW LEP klystron is used in sections 2 and 3, feeding six and four cavity, respectively. That is, each klystron feeds two lattice periods of the intermediate $\beta=0.65$ section and one period of the $\beta=0.85$ section. In order to limit the number of periods fed by a single klystron, for the sake of the machine reliability the first ($\beta=0.5$) section will use 500 kW klystrons, feeding four cavities (two lattice periods).

The energy gain in each cavity is computed from the relation:

$$\Delta V = L_{cav} E_{acc} T(N_{cell}, \beta/\beta_{cav}) \cos(\Phi_{RF}) \quad (1)$$

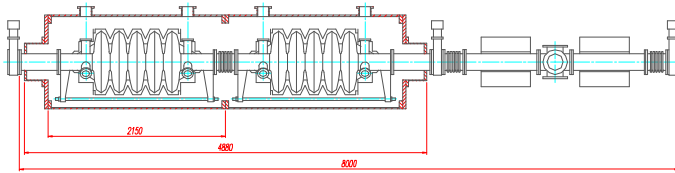
where $L_{cav} = N_{cell} \beta_{cav} \lambda_{rf} / 2$ is the cavity length, E_{acc} is the accelerating gradient (for the synchronous particle), Φ_{RF} is the reference operating phase (-30° in our case) and $T(N_{cell}, \beta/\beta_{cav})$ is the transit time factor of the structure, which depends on the number of cells, N_{cell} , the proton β , and the cavity effective β_{cav} . The choice of the number of cells is determined by the compromise between the increase of active to physical length and the decrease of velocity acceptance, while increasing the number of cells. The active cavity length is also limited by the power transmitted by the couplers. A good compromise within our assumptions and limits is five cell cavities.

The sectioning of the linac in our design resulted in an efficient use of the transit time factor of the cavities, especially in the last section, where most of the cavities operate with a transit time factor of more than 0.95. Only the first modules of each section is allowed to operate at lower values of the transit time factor, down to 0.80, resulting in an overall better efficiency for the whole machine. The particle velocity changes most rapidly at low energies, hence a few cavities in each sections are used for velocity matching by operating them at lower RF power than the rest of the section cavities. This approach allows the totality of each section cavities to operate close to the maximum accelerating gradient, as shown in Fig. 1. Furthermore, the best RF efficiency is set for the majority of cavities at the end of each section, which operate at a constant energy gain. The characteristics of the three sections are given in Table 1, while Figure 2 shows the structure of the lattice periods.

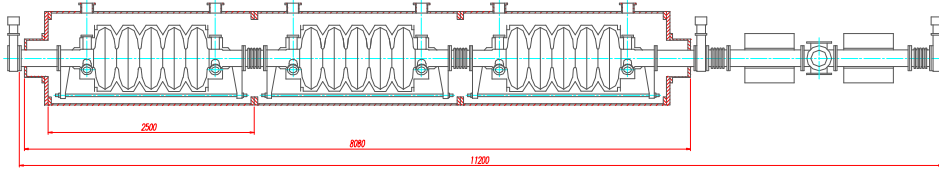
Table 1. Characteristics of the three sections.

Section	1	2	3
Section total length [m]	96	146	475
Injection energy [MeV]	100	190	428
Section period [m]	8	11.2	15.3
# of cavities/section	24	39	124
# of cavities/cryomodule	2	3	4
# of cavities/klystron	4	6	4
Klystron rating (kW)	500	1300	1300

Section at $\beta=0.50$



Section at $\beta=0.65$



Section at $\beta=0.85$

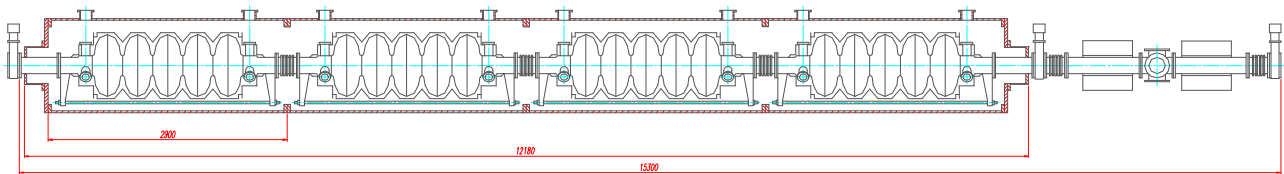


Figure 2. Block layout of the three lattice cells for the three sections of the linac.

The superconducting cavities

A design for bi-elliptical (both at the iris and at the equator) cavity geometry has been carried out and a two year R&D activity to be performed by INFN will be dedicated to the fabrication of copper and niobium prototypes of the cavities. The low $\beta=0.5$ section will use bulk niobium cavities with a proper stiffening structure, for mechanical stability. For the two higher β sections, the sputtering technique will be preferred, in order to reduce the structure costs. A collaboration with CERN[7] is being established to jointly develop a full five cell sputtered cavity for the $\beta=0.85$ section.

A full parametrization of the cavity geometry has been carried out, in terms of parameters such as the iris and equator ellipse axes and the wall side inclination. Our optimizing procedure was aimed at finding a cavity shape with a good coupling between the cells (all the three cavities were designed with a coupling factor of 1.7 %), while maintaining a good performance in terms of the ratio of the peak surface electric and magnetic fields with respect to the accelerating field, and in terms of structural behavior. Different optimization strategies are possible with the chosen parametrization. In particular, the balance between the optimal values for the $E_{\text{peak}}/E_{\text{acc}}$ and $H_{\text{peak}}/E_{\text{acc}}$ ratios, which is driven by the chosen cavity fabrication technology, suggests the final choice of the geometry. This results in the best compromise between the electric and magnetic performances of the cavity.

The operation of the cavities is always limited to a 15 MV/m electric field on the surface, close to the cavity irises, and to a 40 mT magnetic field at the cavity equators.

The β values reported here are the effective β of the cavities, not the geometrical values given by the central cell length $L = \lambda\beta_g/2$. The effective value was defined as the geometrical β value of an ideal (pure sin-like) cavity that results in the same transit time factor curve as that of the actual five cell cavity, including the compensated end cells and drift tubes.

In Table 2 we list the main RF parameters for the three different five cell structures of the linac.

Table 2. Main RF characteristics of the three cavities.

Cavity Parameter	S 1	S 2	S 3
Effective β	0.50	0.65	0.85
$E_{\text{peak}}/E_{\text{acc}}$	3.20	2.60	2.16
$H_{\text{peak}}/E_{\text{acc}}$ (mT/(MV/m))	7.50	6.80	4.90
Max. operating E_{acc} (MV/m)	4.5	5.7	6.6
Max. Energy Gain/Cavity (MeV) at $\Phi_s = -30^\circ$	4.0	6.5	10.0
Coupling Factor (%)	1.7	1.7	1.71

Figure 3 shows the geometry and the fields, computed by SUPERFISH[8], of the $\beta=0.85$ cavity. This cavity has an iris ellipse axes ratio of 1.6, an equatorial ellipse axes ratio of 1.5, the side wall inclination is always greater than 10 degrees (relative to the normal to the cavity axis) and the pipe radius is 11.5 cm, to be reduced to 10 cm at the CF200 flange connection. A copper prototype of this cavity will be built and sputtered with niobium, as part of the R&D on the ADS system.

The end cell geometry has been modified to achieve field flatness, as shown in Figure 4, where is plotted the longitudinal field along the cavity axis.

Preliminary calculations have confirmed, as expected, that the proposed geometry has no limitations induced either by high order modes or multipactoring.

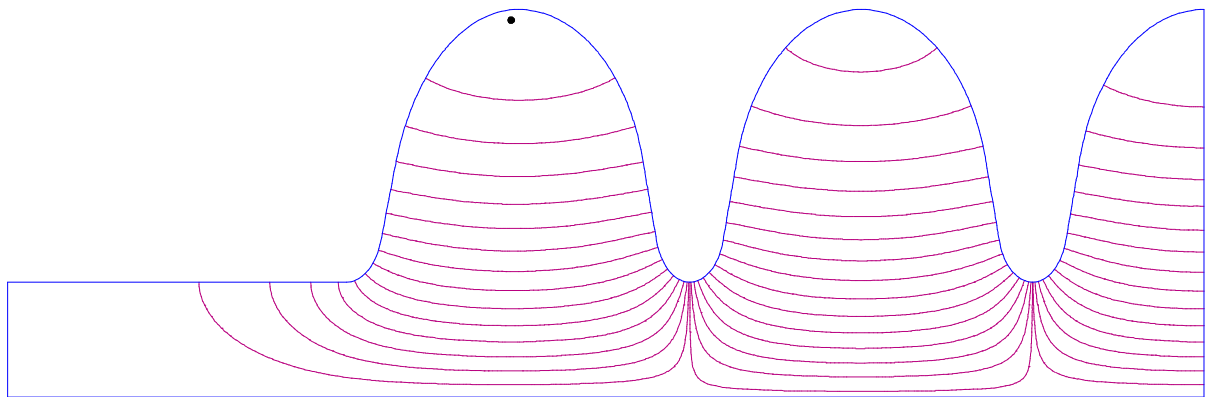


Figure 3. The shape of the $\beta=0.85$ cavity for the third section of the linac (428 to 1600 MeV).

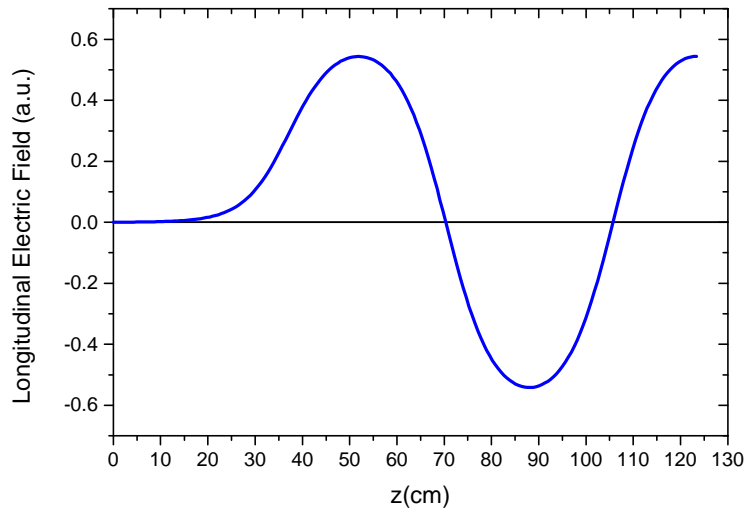


Figure 4. Longitudinal electric field in the $\beta=0.85$ cavity.

Structural behavior of the cavities

Finite Element Analysis (FEA) three dimensional calculations for the mechanical behavior of the cavities under vacuum conditions, performed with the ANSYS code[9], have shown that the low β , bulk Nb, structures will need welded stiffening rings for mechanical stability. Possible stiffening structures have been investigated, and Figure 5 shows an example of the $\beta=0.5$ cavity. Relatively simple stiffening structures that allow for cavity tuning are possible, the stresses being compatible with the Nb yield strength over the whole temperature range of the cavity operation.

No stiffening is required for the $\beta=0.65$ and $\beta=0.85$ cavities.

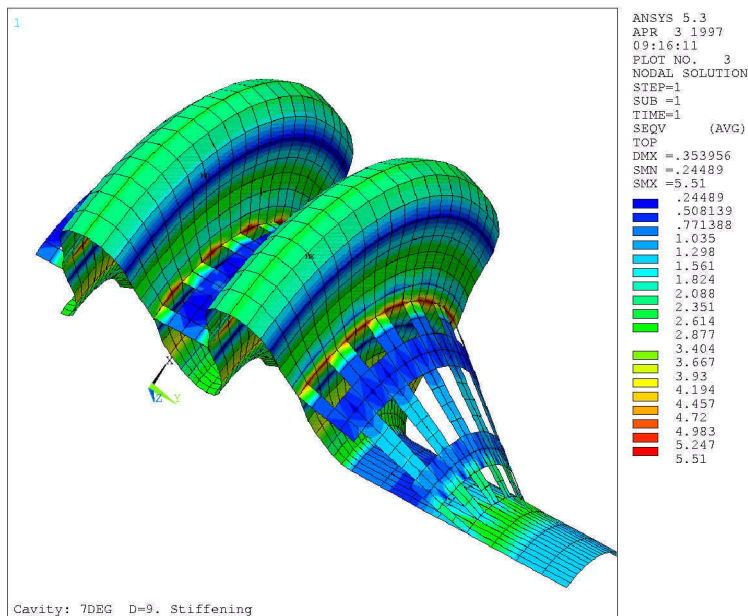


Figure 5. Von Mises equivalent stresses on the stiffened cavity under vacuum operating conditions, at room temperature. The stresses in the welding area are compatible with the yield strength of Nb.

Beam dynamics

The linear beam dynamics have been investigated with the code TRACE3D[10] up to currents of 50 mA. A procedure for matching the beam between the linac sections has been devised, using the energy gain of the last/first cavities of adjacent sections and the doublet gradients at the interface.

The maximum integrated strength (gradient times length) of the quadrupole is of the order of 1.5 T, corresponding to quadrupoles with a physical length of 60 cm (see Fig. 2) and a pole field of 0.5 T.

A normalized emittance of 1π mm mrad (transverse) and 1π deg MeV (longitudinal) has been assumed with a constant synchronous phase $\Phi_s = -30^\circ$. The beam envelopes (horizontal, vertical and longitudinal) for the first ten cells of the last section (from 430 to 780 MeV) are presented in Figure 6 for two extreme cases, i.e. $I = 0$ mA and $I = 50$ mA.

The ratio between the aperture radius and the rms beam size is in excess of 30 everywhere along the linac, assuming a minimum beam pipe radius of 10 cm. Large apertures with respect to the beam size are required to minimize the risk of the linac activation by the halo of the proton beam.

Beam dynamics with a multiparticle space charge code is under development.

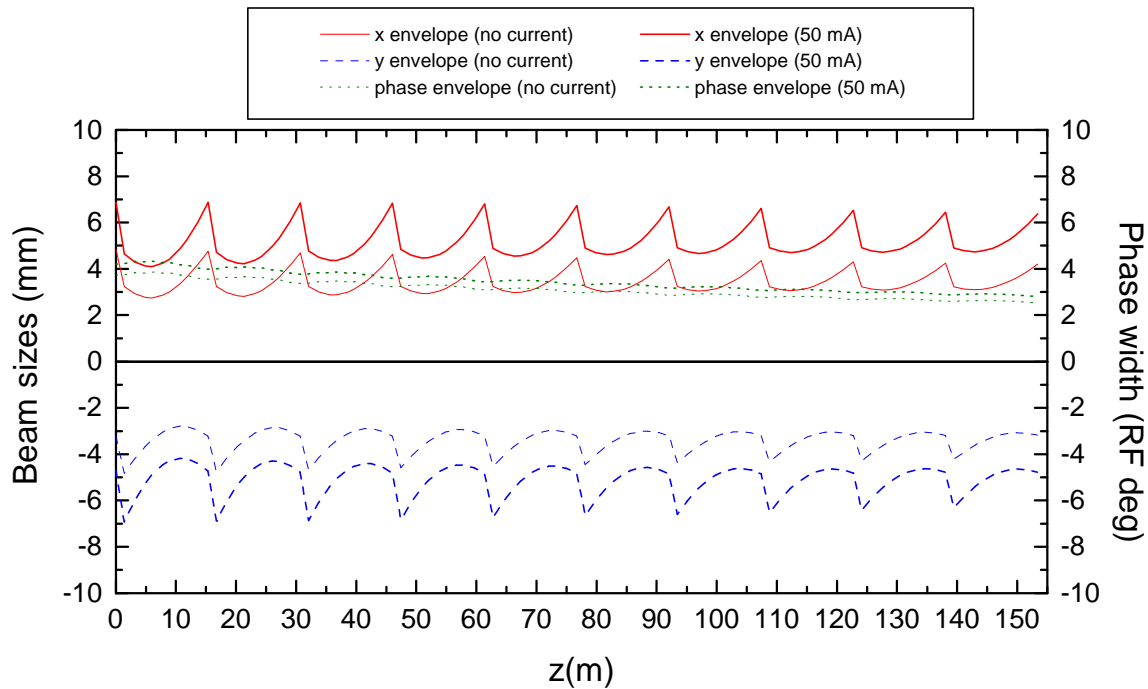


Figure 6. Beam sizes in the first ten cells (430-780 MeV) of the last linac section. The matched envelopes for $I = 0$ mA and for $I = 50$ mA are shown. The solid line is the horizontal envelope, the dashed line is the vertical envelope (shown on the negative side of the axis) and the dotted line is the phase envelope. The wider envelopes correspond to the 50 mA space charge case.

Future R&D program

The objective of the two year program (1998-1999) is to develop crucial components of the superconducting linac and to finalize the design of the ADS system. In particular, we will develop with the industries, niobium monocell $\beta=0.5$ cavities and a complete five cell structure for mechanical and RF warm tests. A complete copper five cell structure at $\beta=0.85$ will be built and sputtered with niobium. After the cold test at CERN[7], in one of the LEP2 vertical cryostats, the cavity should be operated in the horizontal cryostat prototype that we are designing for the linac.

Acknowledgements

We are greatly indebted with Massimo Bonezzi for the technical support.

References

- [1] C. Pagani, G. Bellomo, P. Pierini, "A HIGH CURRENT PROTON LINAC WITH 352 MHZ CAVITIES", Proceedings of the XVIII International Linear Accelerator Conference, editors C. Hill and M. Vretenar, Geneva, August 26-30 1996, CERN 96-07 (1996) p. 107;
- [2] C. Pagani, G. Bellomo, P. Pierini, G. Travish, D. Barni, A. Bosotti, R. Parodi, "A HIGH CURRENT SUPERCONDUCTING PROTON LINAC FOR AN ACCELERATOR DRIVEN TRANSMUTATION SYSTEM", Proceedings of the 1997 Particle Accelerator Conference, Vancouver, May 2-16 1997;
- [3] G. Ciavola, S. Gammino, "A MICROWAVE SOURCE FOR HIGH CURRENT OF PROTONS", LNS-INFN Internal Report, 21/10/96;
- [4] A. Pisent, M. Comunian, G. Fortuna, A. Lombardi, M.F. Moisisio, "THE DTL APPROACH FOR A 100 MEV CW LINAC", LNL-INFN Internal Report 111/96;
- [5] A. Pisent, M. Comunian, "BEAM DYNAMICS ISSUES OF A 100 MEV SUPERCONDUCTING PROTON LINAC", these Proceedings;
- [6] G. Geschonke, "SUPERCONDUCTING STRUCTURES FOR HIGH INTENSITY LINAC APPLICATIONS", Proceedings of the XVIII International Linear Accelerator Conference, editors C. Hill, M. Vretenar, Geneva, August 26-30 1996, CERN 96-07 (1996), p. 910.
- [7] E. Chiaveri, Private Communication;
- [8] Los Alamos Accelerator Code Group, "POISSON/SUPERFISH REFERENCE MANUAL", Los Alamos Report LA-UR-87-126;
- [9] ANSYS is a trademark of SAS IP, Inc;
- [10] K. R. Randall, D. P. Rusthoi, "TRACE 3-D DOCUMENTATION, SECOND EDITION", Los Alamos Report LA-UR-90-4146.